Measurement of the Z_1^3 Contribution to the Stopping Power Using MeV Protons and Antiprotons: The Barkas Effect

L. H. Andersen, P. Hvelplund, H. Knudsen, S. P. Møller, J. O. P. Pedersen, and E. Uggerhøj
Institute of Physics, University of Aarhus, DK-8000 Aarhus C, Denmark

K. Elsener
CERN, CH-1211 Geneva 23, Switzerland

E. Morenzoni
Paul Scherrer Institute, CH-5234 Villigen, Switzerland
(Received 19 January 1989)

The stopping power for antiprotons has been measured for the first time. The antiproton stopping power of silicon is found to be 3%–19% lower than for equivelocity protons over the energy range 3.01 to 0.538 MeV. The "Z_1^3 contribution" to the stopping power (the Barkas effect) is deduced by comparing the stopping power for protons and antiprotons.

PACS numbers: 34.50.Bw, 29.70.Gn, 61.80.Mk

The theory of energy loss of fast charged particles in matter is based on the calculations by Bethe,[1] who derived the stopping power in the first Born approximation. Hence, the Bethe result is proportional to the projectile charge squared, Z_1^2. It was thus a surprise when Barkas, Birnbaum, and Smith[2] found that the range of negative pions was longer than that of positive pions of equal momentum. Barkas, Dyer, and Heckman[3] suggested that the effect was due to a difference in the stopping power stemming from the opposite charge of the particles. The reduction in the stopping power, responsible for the longer range of negative particles as compared to their positively charged antiparticles was later investigated with sigma hyperons,[3] pions,[4] and muons,[5] but these measurements all suffered from the poor quality of the low-velocity particle and antiparticle beams used.

This so-called Barkas effect has been interpreted as a polarization effect in the stopping material depending on the charge of the projectile. It appears as the second term (proportional to Z_1^3) in the implied Born expansion of the energy loss. The Barkas correction was first calculated by Ashley, Ritchie, and Brandt[6] using a classical perturbation calculation for a harmonic oscillator. The effect originates in the nonnegligible displacement of the atomic electron during the collision. Their calculation only applies for distant collisions, but the authors assert that the close collisions are essentially those of free particles, giving an exact Z_1^2 dependence. The minimum impact parameter for distant collisions, of major importance for the result, was used as an adjustable parameter to fit experimental data. At the same time, Jackson and McCarthy[7] performed a similar, but relativistic, calculation arriving basically at the same conclusions, but they chose the minimum impact parameter as the radius of the harmonic oscillator in question. Subsequently, Lindhard[8] argued that there is an equally important contribution to the Z_1^3 term from the close collisions, which are *not* exactly Coulomb-like due to dynamical screening of the projectile charge by the atomic electrons. This contribution was estimated to be comparable to the distant-collision contribution as calculated by Jackson and McCarthy and improved the agreement between experimental data and the Ashley-Ritchie-Brandt theory. Subsequently, Ritchie and Brandt[9] obtained equally good agreement with the data without recourse to a close-collision contribution by adjusting their impact-parameter cutoff. Many other calculations of the Barkas effect have appeared, but the principal disagreement is still on the significance of the close-collision contribution to the Barkas effect.

On the experimental side, deviations from a strict Z_1^2 dependence of the stopping power were also seen when stopping powers for protons and α particles were compared.[10] However, to extract the Z_1^3 correction, it was necessary to include data for particles of charge other than +1 and +2, for example, Li nuclei,[11] since the Z_1^4 term in the Born expansion of the stopping power is nonnegligible for projectile velocities of a few atomic units.[8] The magnitude of the Barkas term in the stopping power as extracted from H^+, He^{2+}, and Li^{3+} particle data[11] agrees essentially with the assesment by Lindhard, as well as with Ritchie and Brandt. However, the analysis is somewhat hampered by a possible modification of the effective charge of the Li projectiles caused by electron capture. It is therefore essential that the magnitude of the Barkas term be determined in an alternative way.

In light of the above discussion of the theoretical treatment of this effect, it is not possible to deduce the significance of the close collisions from the magnitude of the Barkas term only, but detailed experiments are needed to provide guidelines for further theoretical developments. For recent reviews of the experimental and theoretical situation, see Refs. 12 and 13.

With the advent of the low-energy antiproton ring

(LEAR) at CERN, high-quality beams of antiprotons at low energy became available, making an accurate comparison of stopping powers for antiprotons and protons feasible. The present experiment was performed with the 105.5-MeV/c (5.91 MeV kinetic energy) LEAR beam, which had an intensity of $\sim 10^4$ sec^{-1} and a momentum spread of $\sim 10^{-3}$. The beam exits from the LEAR ultrahigh vacuum system through a ~ 100-μm Be window, passes through ~ 2 cm of air, and enters the experimental vacuum chamber through a 22-μm Mylar foil. Next, the beam traverses a 100-μm scintillator (start), which together with another scintillator (stop) ~ 1 m downstream is used to measure the time of flight (TOF) of the beam particles. Lower proton and antiproton energies were obtained by inserting various aluminum degrader foils in the air between the two vacuum systems. For each degrader, TOF spectra were recorded with the stop scintillator at two positions, separated by an accurately determined distance of 0.5 m. The time resolution of the system, determined as the FWHM of the TOF distribution of the undegraded beam, was 2.4 ns corresponding to an energy resolution (FWHM) of 24% at 3 MeV and 9% at 0.6 MeV. The position of the peak of the TOF distribution, which was used to calculate the beam energy, could be deduced much better, leading to a determination of the beam energy within 1%.

The energy loss of the particles was measured as the energy deposited in either of two thin transmission silicon detectors, 6.9 and 2.9 μm thick, respectively. The energy deposited in the semiconductor detector is mainly spent in forming a number of electron-hole pairs, which is closely proportional to the energy absorbed. The charge produced is extracted by the applied bias and subsequently amplified. The electronical noise of the detector-amplifier system was 14.6 and 18.4 keV (FWHM), respectively, which is less than the energy straggling in the detectors. The contribution to the energy resolution from the statistics of the produced electron-hole pairs is negligible. For beams degraded to less than 2 MeV, the energy straggling from the degrader dominates over the straggling in the silicon detector. There is a difference between the energy lost by the particles and the energy deposited in the Si detector, which is measured. This difference is mainly caused by the escape of δ rays, but as discussed in Ref. 11, the corrections amount to less than a few times 10^{-3}. Since the Si detector is a single crystal, channeling may change the energy loss.[14] By tilting the detector slightly around perpendicular beam incidence, it was assured that the energy-loss spectra obtained were without any significant influence from channeling. To exclude the edge of the detector, the signals from the 10-mm^2 transmission detectors were gated with a 7-mm^2-thick Si detector mounted behind the ΔE detector. An electronic pulser and a polonium α source assured stability of the amplifier system.

As an example, Fig. 1 shows an energy-loss spectrum from the 6.9-μm ΔE detector for 3.01-MeV incident antiprotons. A small background from annihilation products is visible. The energy-loss distribution is slightly asymmetric with a small high-energy-loss tail, and is of the Vavilov type, since the parameter characterizing the distribution function, $\kappa = \xi / E_{\max}$, is of the order of unity.[15] Here $\xi = 2\pi e^4 \Delta x N Z_2 / m v^2$ and the maximum energy transfer $E_{\max} = 2mv^2$, where Δx is the target thickness, N is the target density, Z_2 is the target atomic number, v is the projectile velocity, and m and e are the electron mass and charge, respectively. The tail in the energy-loss distribution is included in the extraction of the *average* energy loss.

The stopping power is determined as the average energy loss divided by the target thickness, $\Delta E / \Delta x$, at the mean energy $\bar{E} = E_0 - \Delta E/2$, where E_0 is the incident particle energy. Multiple scattering can be neglected, as the average path length of the particles in the target is less than 0.2% larger than the actual target thickness. To calibrate the ΔE detector, proton stopping powers were measured at a few energies. The proton reference beams of 1.55–3.40 MeV were also obtained by degradation of a 105.5-MeV/c beam from LEAR. The calibration constant was found by requiring the measured proton stopping powers to agree with the recommended values by Andersen and Ziegler.[16] The measured stopping powers for protons and antiprotons for the two ΔE detectors are shown in Fig. 2. We observe that the measured proton stopping power follows the solid curve (from Ref. 16) to better than 1%, giving confidence in the method used. It is also seen that the measured antiproton stopping power is lower than that of protons, as expected. The difference is 3% at 3.01 MeV and 19% at 0.538 MeV. Finally, there is consistency between the measurements with the two ΔE detectors.

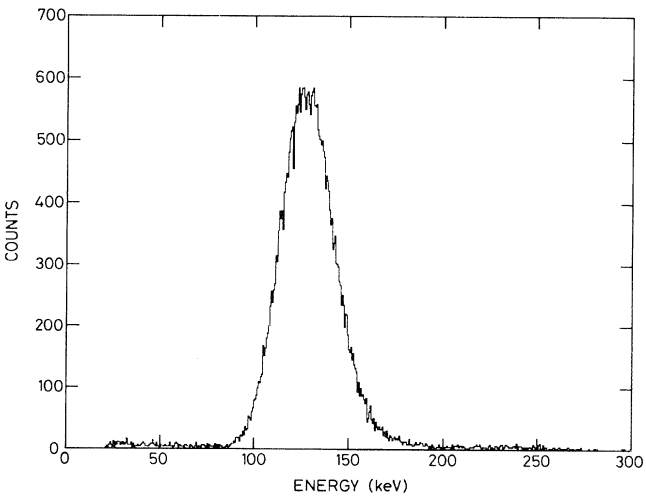

FIG. 1. Energy-loss spectrum for 3.01-MeV antiprotons traversing the 6.9-μm Si detector.

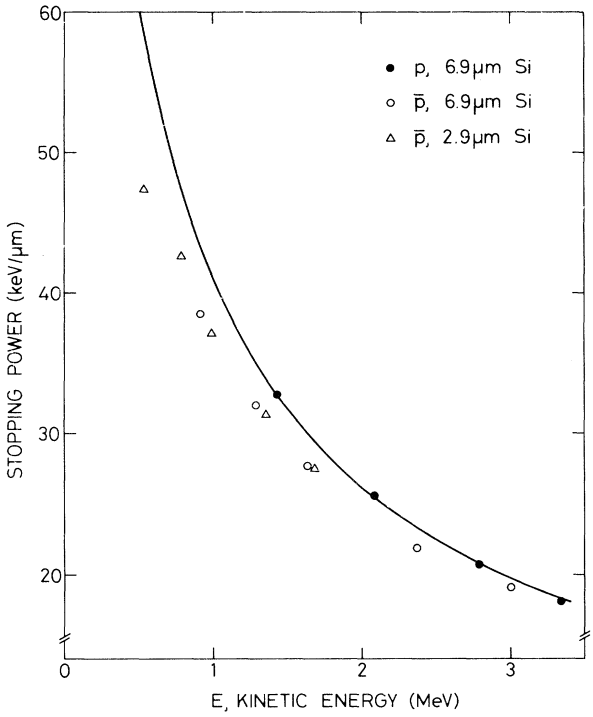

FIG. 2. Measured stopping power of Si for protons and antiprotons from this work. The solid curve is the recommended stopping power for protons from Ref. 16.

The main feature of Fig. 2 is, however, the uninteresting $1/v^2$ dependence of the stopping power. The Bethe result for the stopping power is given by

$$-dE/dx=(4\pi e^4NZ_2/mv^2)Z_1^2L_0\,, \tag{1}$$

where the Bethe stopping function L_0, which is independent of Z_1, may be written

$$L_0=\ln[2mv^2/I(1-\beta^2)]-\beta^2-C/Z_2\,, \tag{2}$$

$\beta=v/c$ being the projectile velocity relative to the velocity of light c, I the mean ionization potential, and C/Z_2 the so-called shell corrections.

Formally, one may generalize the above stopping-power formula, Eq. (1), by including higher-order Z_1 terms in the stopping function,

$$L=L_0+Z_1L_1+Z_1^2L_2\,, \tag{3}$$

where L_1 and L_2 are the Z_1-independent coefficients of the Z_1^3 and Z_1^4 terms in the stopping power, and where higher-order terms are omitted. Z_1L_1 is the Barkas term and $Z_1^2L_2$ includes the so-called Bloch correction, which marks the transition to the classical scattering regime. To elucidate the interesting part of the measured stopping powers, we plot in Fig. 3 the so-called reduced stopping power X, which is the stopping power reduced by

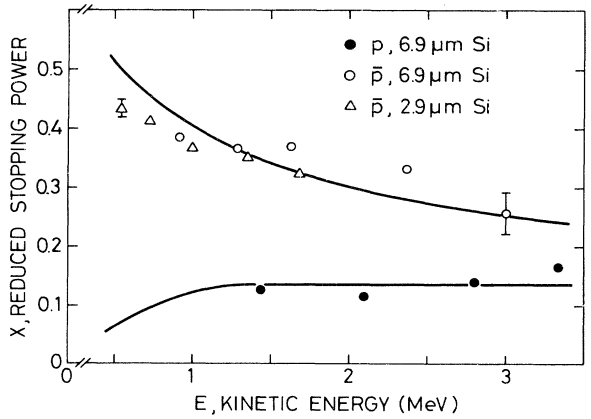

FIG. 3. Reduced stopping power, Eq. (4), of Si for protons and antiprotons. The solid curves show the reduced stopping power from Ref. 16, the upper curve including the Barkas effect corresponding to twice the Jackson-McCarthy result (Ref. 7).

the trivial factors, defined by

$$X=\ln\left(\frac{2mv^2}{I(1-\beta^2)}\right)-\beta^2-\frac{mv^2}{4\pi e^4NZ_2Z_1^2}\left(-\frac{dE}{dx}\right)$$
$$=\ln\left(\frac{2mv^2}{I(1-\beta^2)}\right)-\beta^2-L\,. \tag{4}$$

We have used the value $I=165$ eV (Ref. 16). The theoretical reduced stopping power is now given as

$$X_{\text{theor}}=C/Z_2-Z_1L_1-Z_1^2L_2\,. \tag{5}$$

The two curves in Fig. 3 represent the reduced stopping power from Ref. 16 (protons) and the same stopping power corrected for the Lindhard Z_1^3 term[8] corresponding to twice the Jackson and McCarthy value.[7] The difference in the measured stopping for protons and antiprotons is now clearly visible. The error bars correspond to $\pm 1\%$ on the stopping power, which is the estimated uncertainty. The proton measurements agree with the recommended curve (Ref. 16) within the uncertainty. The measured antiproton stopping powers are in reasonable agreement with the Lindhard result, as well as with that of Ritchie and Brandt, especially for the high-energy points.

Finally, in Fig. 4 we have extracted the Barkas term L_1 from the data, as one-half the difference between the proton stopping power from Ref. 16 and the measured antiproton stopping power. The results are plotted here as a function of the velocity in units of the Bohr velocity $v_0=\alpha c$, $\alpha=e^2/\hbar c$ being the fine-structure constant. The error bars stem from the $\pm 1\%$ uncertainty on the stopping-power measurement. The solid curve is the Jackson and McCarthy result (Ref. 7) and the dashed line is twice the result of this calculation as suggested by Lindhard.[8] The measurements coincide with the latter

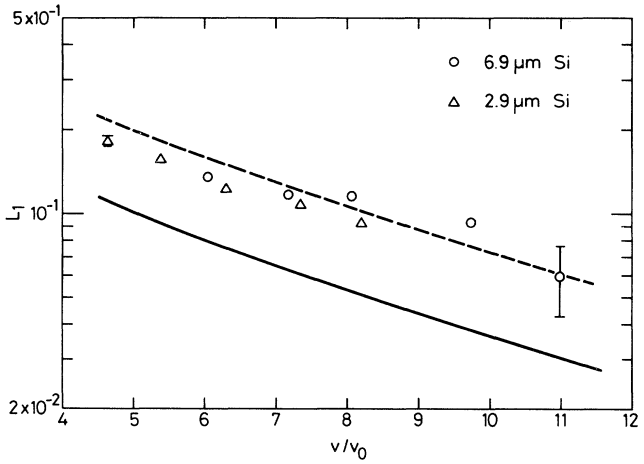

FIG. 4. The Z_1^3 contribution, L_1, to the stopping power extracted from the measurements. The solid and dashed curves correspond to the Jackson-McCarthy result and twice this value, respectively.

curve for the higher velocities, but there seems to be a tendency for the measured points to fall slightly below the curve for the lower velocities. In particular, the calculated velocity dependence of L_1 ($\propto v^{-1.7}$ in the considered velocity range) essentially reproduces the observed one ($\propto v^{-2}$). Consequently, the measured Barkas term is around a factor of 2 larger than that calculated by Jackson and McCarthy for the distant collisions only, and in close agreement with the estimate of the Barkas term by Lindhard[8] with roughly equal contributions from close and distant collisions. We note, however, that the Ritchie-Brandt theory[9] is in equally good agreement with the data.

In Ref. 17, some of us observed an increased double-ionization cross section for antiprotons in noble gases as compared to proton impact. It was demonstrated that such an effect, which is not included in any calculations of stopping power, leads to a nonnegligible contribution to the Barkas effect of opposite sign to that of polarization effects. This effect could also play a role for solids, such as silicon.

Earlier experiments,[4,5,11] on targets other than silicon, have shown indications of a Z_1^3 contribution to the stopping power of slightly larger magnitude than reported here, but experimental uncertainties or uncertainties in the interpretation of the data have prevented a clear estimate of the L_1 term.

There is an interest in extending the present measurements to lower antiproton velocities and to other targets. The simplicity and accuracy of the present method in obtaining relative stopping powers for antiprotons and protons relies on the target being a semiconductor detector. For other targets, the antiproton energy would have to be measured before and after the target. For energies lower than 0.5 MeV, with the present minimum momentum of 105 MeV/c from LEAR, this would have to be done on an event-by-event basis due to the large straggling from the degrader.

[1]H. A. Bethe, Ann. Phys. (Leipzig) **5**, 325 (1930); U. Fano, Annu. Rev. Nucl. Sci. **13**, 1 (1963).

[2]W. H. Barkas, W. Birnbaum, and F. M. Smith, Phys. Rev. **101**, 778 (1956).

[3]W. H. Barkas, N. J. Dyer, and H. H. Heckman, Phys. Rev. Lett. **11**, 26 (1963).

[4]H. H. Heckman and P. J. Lindstrom, Phys. Rev. Lett. **22**, 871 (1969).

[5]W. Wilhelm, H. Daniel, and F. J. Hartmann, Phys. Lett. **98B**, 33 (1981).

[6]J. C. Ashley, R. H. Ritchie, and W. Brandt, Phys. Rev. B **5**, 2393 (1972); Phys. Rev. A **8**, 2402 (1973).

[7]J. D. Jackson and R. L. McCarthy, Phys. Rev. B **6**, 4131 (1972).

[8]J. Lindhard, Nucl. Instrum. Methods **132**, 1 (1976).

[9]R. H. Ritchie and W. Brandt, Phys. Rev. A **17**, 2102 (1978).

[10]H. H. Andersen, H. Simonsen, and H. Sørensen, Nucl. Phys. **A125**, 171 (1969).

[11]H. H. Andersen, J. F. Bak, H. Knudsen, and B. R. Nielsen, Phys. Rev. A **16**, 1929 (1977).

[12]H. H. Andersen, in *Semiclassical Descriptions of Atomic and Nuclear Collisions,* edited by J. Bang *et al.* (Elsevier, New York, 1985), p. 409.

[13]G. Basbas, Nucl. Instrum. Methods B **4**, 227 (1984).

[14]H. Esbensen *et al.*, Phys. Rev. B **18**, 1039 (1978).

[15]H. Bichsel, Rev. Mod. Phys. **60**, 663 (1988).

[16]H. H. Andersen and J. F. Ziegler, *Hydrogen Stopping Powers and Ranges in All Elements* (Pergamon, New York, 1977).

[17]L. H. Andersen, P. Hvelplund, H. Knudsen, S. P. Møller, A. H. Sørensen, K. Elsener, K.-G. Rensfelt, and E. Uggerhøj, Phys. Rev. A **36**, 3612 (1987).